Magnetic circular dichroism of resonant x-ray emission spectroscopy for Sm $L_3M_{4,5}$ and L_2M_4 in a $Sm_{21}Co_{79}$ amorphous alloy

Tetsuya Nakamura,* Hironobu Shoji, Eiju Hirai, and Susumu Nanao
Institute of Industrial Science, University of Tokyo, Tokyo 153-8505, Japan

Keiji Fukui,† Haruhiko Ogasawara, and Akio Kotani
Institute for Solid State Physics, University of Tokyo, Kashiwa, Chiba 277-8581, Japan

Toshiaki Iwazumi
Photon Factory, Institute of Materials Structure Science, 1-1 Oho, Tsukuba 305-0801, Japan

Isao Harada
Department of Physics, Faculty of Science, Okayama University, Okayama 700-8530, Japan

Rintaro Katano and Yasuhito Isozumi
Radioisotope Research Center, Kyoto University, Kyoto 606-8501, Japan

(Received 18 September 2002; revised manuscript received 13 December 2002; published 31 March 2003)

The magnetic circular dichroism (MCD) of resonant x-ray emission spectroscopy (RXES) was studied for the Sm $L_3M_{4,5}$ and L_2M_4 optical processes in a ferromagnetic $Sm_{21}Co_{79}$ amorphous alloy. The MCD of RXES (MCDRXES) originating from the optical process of $2p^63d^{10}4f^n \rightarrow 2p^53d^{10}4f^{n+1} \rightarrow 2p^63d^94f^{n+1}$, which corresponds to dipolar decay after quadrupolar ($E2$) excitation, was obviously observed at the preedge region in addition to that of the normal dipolar ($E1$) excitation. Moreover, the $E2$ contribution of the MCD has been separated into those for $E2$ excitation to the Sm $4f$ state with majority and minority spins. A theoretical calculation based on a formula of the coherent second-order optical process was carried out for all of the experimental MCDRXES spectra. In the calculation, the multiplet coupling effect and the enhancement of the $2p$-$5d$ dipole matrix elements proposed for the MCD of x-ray absorption were taken into account. The calculated MCDRXES spectra reproduced all of the experimental results very successfully. The present result provided an appropriate interpretation of the origins of the MCD effect, which comes from the $E1$ and the $E2$ contributions at both the L_3 and the L_2 edges.

DOI: 10.1103/PhysRevB.67.094439 PACS number(s): 87.64.Ni, 71.20.Eh, 78.70.En

I. INTRODUCTION

X-ray magnetic circular dichroism (MCD) has been developed as the powerful probe to investigate ferromagnetic and ferrimagnetic materials with element and shell selectivity in the last decade. MCD at the rare-earth (RE) $L_{2,3}$ edges has been measured to study the magnetic behavior of the $5d$ spins, which play essential roles in the indirect $3d$-$4f$ exchange interaction in RE transition-metal systems.[1] The information on the $5d$ spin state obtained from the MCD should be very precious, because no other experimental means can reflect the $5d$ magnetism more directly. Despite this principal benefit, the interpretation of MCD at the RE $L_{2,3}$ edges has been debated due to some secondary effects, such as the presence of a quadrupolar ($E2$) transition,[2–10] the spin dependence of the radial parts of the matrix elements[11,12] and, more recently, $3d$-$5d$ band mixing in RE-transition metal systems.[13] Among them, a confirmation of the existence of the $E2$ contribution has been a controversial subject in the MCD studies at the RE $L_{2,3}$ edges for a long time. The preedge structure of the MCD spectra could be regarded as the $E2$ transition to the $4f$ state from the $2p$ core state, because the $4f$ level is pulled down below the $2p$-$5d$ absorption edge due to the strong Coulomb interaction between the $2p$ core hole and the $4f$ electrons.

Some early reports have discussed the θ dependence of the MCD intensities, where θ is the angle between the spin vector and the incident x-ray beam. The θ dependence is given as

$$\mu_c^{E1} = \frac{6\pi N}{k}(w_{11} - w_{1-1})\cos\theta, \tag{1}$$

$$\mu_c^{E2} = \frac{10\pi N}{k}[(w_{22} - w_{2-2})\sin^2\theta + (w_{21} - w_{2-1})\cos 2\theta]\cos\theta, \tag{2}$$

where N is the number of atoms per unit volume, w_{lm} are the matrix elements of the transition, and μ_c^{E1} and μ_c^{E2} are the MCD intensities for the $E1$ and the $E2$ excitations.[2] Equation (1) means that μ_c^{E1} is proportional to $\cos\theta$, while μ_c^{E2} deviates, as found from Eq. (2), from the proportional dependence to $\cos\theta$. In an early stage of verifications based on Eqs. (1) and (2), several experiments[3–7] were tested at room temperature and failed to find the existence of the $E2$ contribution in the MCD spectra because the deviation of the angular dependence of $E2$ MCD from $\cos\theta$ decreases with increasing temperature due to thermal fluctuation. In 1995,

Lang *et al.* confirmed the existence of the $E2$ contribution at the Dy L_3 edge of a $Dy_{0.6}Tb_{0.4}$ alloy cooled down to 80 K.[8] However, the result of a similar study in $YbFe_2$ by Giorgetti *et al.*[9] seems not to be consistent with a resonant x-ray emission spectroscopy (RXES) study in $Yb_2Fe_{14}B$ by Bartolomé *et al.*[14] with respect to the energy at which $E2$ MCD appears. The latter study in $YbFe_2$ convinced us of the limitation of confirming the existence of the $E2$ MCD experimentally by means of x-ray-absorption spectroscopy (XAS) .

RXES has remarkably progressed thanks to the development of highly brilliant synchrotron x-ray sources. RXES is a coherent second-order optical process, and gives more detailed information on the solid-state physics than the first-order ones, such as XAS (Ref. 15) or x-ray photoemission spectroscopy. Since the optical process is identified by the emission energy in RXES, the $E2$ contribution can be separated from $E1$, judging from the energy scheme.[16–20] The signature of the $E2$ transition is visible in RXES as an independent peak originating from optical processes, $2p^63d^{10}4f^n \rightarrow 2p^53d^{10}4f^{n+1} \rightarrow 2p^63d^94f^{n+1}$. From this point of view, the MCD of RXES (MCDRXES) is just a direct and powerful probe to investigate the $E2$ contribution of MCDXAS (MCD spectra of XAS) in spite of the weakness in the MCDRXES signal intensity.

The MCDRXES of Gd $L_3M_{4,5}$ was observed in a metallic Gd by Krisch *et al.* for the first time,[21] where $L_3M_{4,5}$ represents the x-ray emission of the decay from $M_{4,5}$ shells after L_3 absorption. The fluorescent $L_3M_{4,5}$ and L_2M_4 emission lines, which were investigated in this work, have been conventionally called $L\alpha_{1,2}$ and $L\beta_1$. The MCDRXES of the $L_3M_{4,5}$ for Gd,[22–27] Ho,[28] and of the $L_3M_{4,5}$ for La, Sm, and Gd,[29] and of the $KL_{2,3}$ for Co (Ref. 30) have been studied by the present authors. A theoretical calculation taking into account multiplet interactions well reproduced the experimental MCD spectra for the off-resonant XES of the Gd $L_3M_{4,5}$ by de Groot *et al.*[31] and L_2M_4, $L_3M_{4,5}$, $L_3N_{4,5}$, L_2N_4 for Nd, Gd, and Dy ions by Jo and Tanaka.[32] As same as conventional RXES, MCDRXES is a favorable approach to elucidate the $E2$ contribution in MCDXAS. Actually, the $E2$ contribution has been observed in MCDRXES of $L_3M_{4,5}$ in Gd (Refs. 21 and 22) and Ho (Ref. 28) when the incident x-ray energy is tuned to the preedge region, though they have not yet been confirmed by theoretical calculations.

In this paper, the MCDRXES for the Sm $L_3M_{4,5}$ and L_2M_4 in a $Sm_{21}Co_{79}$ amorphous alloy is presented along with a comparison between the experimental and calculated spectra. The ferromagnetic Sm ion was chosen as the typical and preferable element for a MCDRXES study. The Sm MCDXAS at the L_3 edge shows a complicated feature due to a strong superposition between the $E1$ and $E2$ contributions, as shown in the following experimental section. The present study covered both the L_3 and L_2 edges, because the $E2$ contribution of MCD at the L_2 edge, at which the MCD intensity is larger than that at the L_3 edge, has been reported less so far, also, it is very interesting to investigate the details by means of RXES. Theoretical calculations were performed for all of the experimental MCDRXES spectra based on an appropriate model, which had already been established in the previous work for the Gd $L_3M_{4,5}$ and L_2M_4 MCDRXES.[26,27,33]

II. EXPERIMENTS

A ferromagnetic $Sm_{21}Co_{79}$ amorphous thin film of 2 μm thickness was prepared by deposition onto a polyimide film with rf magnetron sputtering. The surface of the thin film was coated with a Si_3N_x layer (20 nm) to prevent oxidization. MCDXAS and MCDRXES experiments were performed at the elliptical multipole wiggler beamline 28B of the Photon Factory, Institute of Materials Structure Science.[34] The incident x rays with minus helicity were monochromatized using Si (111) reflection, where the estimated degrees of circular polarization (P_c) were 0.53 and 0.51 at the Sm L_2 and L_3 edges, respectively. The MCD spectra of XAS in $Sm_{21}Co_{79}$ at the Sm $L_{2,3}$ edge were measured at room temperature with the transmission geometry using two ion chambers. Instead of switching the helicity of the incident photons, an applied magnetic field of about 0.6 T was reversed every 4 s to obtain the MCD effect. The surface of the sample was parallel to the applied magnetic fields, and was tilted by 45° along the wave vector **k** of the incident beam. MCD is given as $\mu_+(\omega_1)-\mu_-(\omega_1)$, where $\mu_+(\omega_1)$ and $\mu_-(\omega_1)$ correspond to the XAS spectra when the angle between **k** and the magnetic field is acute and obtuse, respectively; ω_1 and ω_2 are the energies of the incoming and outgoing x rays, respectively.

The geometrical layout of the MCDRXES experiment has already been introduced in Ref. 30, where the angle between the scattered x rays and the normal of sample surface was set to 54.7°. The angle between the incident x rays and the sample magnetization (θ) was chosen to be 36.9° to obtain the best compromise between the energy resolution of the emission spectra and the magnitude of the MCD signals. It should be noticed that θ is different from that for the experiment of MCDXAS due to a geometrical limitation of the present experimental setup. A magnetic field of 1.1 T was applied to the sample using a magnetic circuit made of a pair of Nd-Fe-B permanent magnets, and the field direction was switched every 10 s to obtain the MCD effect without changing the helicity of the incident x rays. Cylindrical bent InSb (440) and Ge (333) crystals were used to analyze the emitted x rays for the Sm $L_3M_{4,5}$ and the L_2M_4, respectively. The analyzed x rays were counted by a position-sensitive proportional counter filled with an Ar + 10% CH_4 mixture of 7 atm. The total-energy resolutions of the present apparatus were 1.2 eV and 1.3 eV around Sm $L_3M_{4,5}$ and the L_2M_4 fluorescence lines, respectively. MCDRXES was defined as $I_+(\omega_2)-I_-(\omega_2)$, where $I_+(\omega_2)$ and $I_-(\omega_2)$ are the intensities of the fluorescence yield. They were measured when the **k** of the incident beam was parallel and anti parallel to the magnetization of the sample, respectively.

Figure 1 shows XAS spectra and MCDXAS at the Sm L_3 and the L_2 edges in the $Sm_{21}Co_{79}$ amorphous thin film. The intensity of the spectra was corrected by the factor $P_c\cos\theta$. This correction was not exact for the $E2$ part of the MCD, but almost true, because the spectra were measured at room

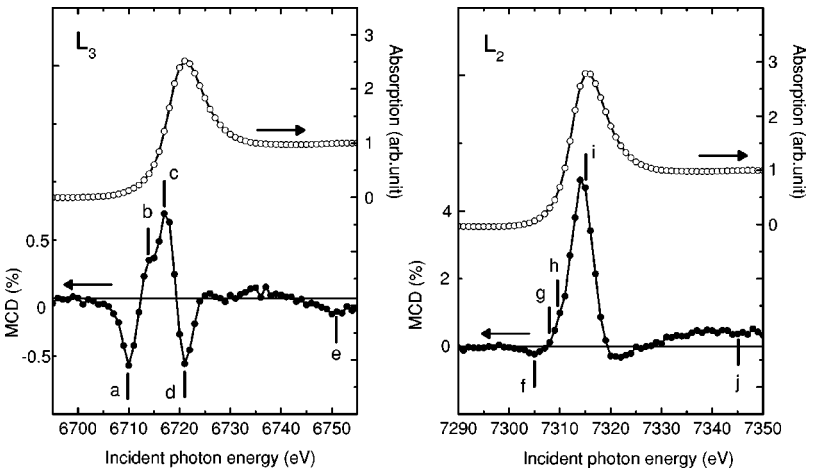

FIG. 1. XAS spectra (open circle) and MCD (filled circle) at the Sm L_3 edge ($left$) and the L_2 edge ($right$) in $Sm_{21}Co_{79}$ amorphous thin film at room temperature. The MCDRXES were measured at the energies labeled by $a-e$ for the L_3 edge and $f-j$ for the L_2 edge with vertical lines.

temperature, at which the confirmation of the $E2$ MCD based on Eq. (2) has not yet been successfully made. Peaks *a* and *b* on the MCDXAS spectrum at the L_3 edge, which have opposite signs and are located in the preedge region, are attributed to the $E2$ transition to the majority and minority spins of the $4f$ state, respectively. Peaks *c* and *d* of the $E1$ character correspond to the first inflection point and the white line of XAS spectrum, respectively. As at the Sm L_3 edge, the energies labeled *f*, *i*, and *j* in MCDXAS at the L_2 edge represent the $E2$ contribution, the white line and off resonant region of XAS, respectively. The energies labeled $a-j$ in Fig. 1 were chosen as those at which the RXES spectra were measured, where the energy labeled *e* and *j* can be regarded as an off-resonant region. According to a theoretical investigation by Fukui *et al.*, the $3d-5d$ band mixing is likely to be reflected at energy *c* and *h* on the MCDXAS spectrum[13]. The magnitude of MCDXAS at the L_2 edge is about 6-times as large than that of the L_3 edge, which is a typical tendency for MCDXAS of the light RE group.

The RXES spectra of Sm $L_3M_{4,5}$ and the L_2M_4 are shown in Fig. 2 as the ω_1 dependence. In the following discussion on the overall feature of RXES, the experimental result at the L_3 edge focuses on the intense L_3M_5 feature due to the inherent weakness of the L_3M_4 emission. The ω_1 dependence of the RXES intensity correctly followed XAS at the L_3 and L_2 edges except for a deviation due to a self-absorption effect (not shown here). In the RXES spectra for $\omega_1=6704$–6712 eV, the $E2$ emission lines labeled Q_1 are observed, which can be explained as the $E1$ emission of the $3d2p$ decay after the $E2$ transition to the $4f$ majority level. The energy difference of ω_2 between the $E1$ and the Q_1 is about 9.0 eV. Around an incident energy of 6711 eV, the Raman shift for Q_1 appears to be saturated. The shoulder structure labeled Q_2 can be seen on the RXES spectra for $\omega_1=6710$–6714 eV, which corresponds to the $E2$ contribution related to the $4f$ minority level. The energy deviation of Q_2 from the $E1$ emission line is about 5.0 eV for $\omega_1=6714$ eV. As for $E1$, a Raman shift is clearly observed in the spectra below $\omega_1=6721$ eV; small peaks originating from the off-resonant Raman scattering are also visible above $\omega_1=6728$ eV, where the Raman scattering corresponds to the transition into the $5d$ state. On the other hand, fluorescence is dominated for the RXES spectra above $\omega_1=6721$ eV, where the fluorescence originates from the transition into the continuum state above the $5d$ band. For Sm L_2M_4, the overall $E1$ feature, such as the existence of a Raman shift, is consistent with those for $L_3M_{4,5}$. As in the case of $L_3M_{4,5}$, the $E2$ feature is also observed at 6.8 eV above the $E1$ emission line in the RXES spectra for $\omega_1=7302$ and 7308 eV.

The MCDRXES spectra measured for $L_3M_{4,5}$ and L_2M_4 are shown in Fig. 3. In the MCDRXES spectrum at (a) in Fig. 3, the $E2$ MCD features associated with Q_1 and Q_2 are observed with negative and positive signs, respectively. The signs of peaks Q_1 for Fig. 3(a) and the Q_2 for 3(b) are consistent with those of the MCDXAS at the corresponding ω_1. For the MCDRXES of Q_1, the $E2$ contribution is confirmed to be the dominant origin of the corresponding MCDXAS because the $E1$ part has a dispersive shape, whose integration seems to be almost zero. The $E2$ contribution of the MCDRXES of L_3M_4 is also observed at $\omega_2=5610$ eV, which has almost a comparable intensity with the $E1$ part of L_3M_4. The MCDRXES spectrum becomes very narrow at $\omega_1=6717$ eV due to the resonance of the $E1$ transition.

For L_2M_4, the signs of the $E1$ part of the spectra are inverted with respect to those for L_3M_5. The magnitude of MCDRXES for L_2M_4 is almost similar to that for L_3M_5 in spite of a huge difference of the intensity in MCDXAS, where MCDXAS can be regarded as approximately the integration of MCDRXES. The large difference in MCDXAS is attributed to subtle unbalances in the intensity between the positive and negative peaks of the MCDRXES spectra. The $E2$ MCD feature can also be seen in (f) and (g) of Fig. 3, which has a negative sign. As in the case of MCDRXES for the L_3M_5, the signs for L_2M_4 are consistent with those of MCDXAS at the corresponding ω_1 in Fig. 1. MCDRXES spectrum is sharpened at $\omega_1=7315$ eV, which is in the resonance condition of the $E1$ transition.

III. MODEL OF THE CALCULATION AND THE RESULT

We used a formula of the coherent second-order optical process for RXES, which is represented by

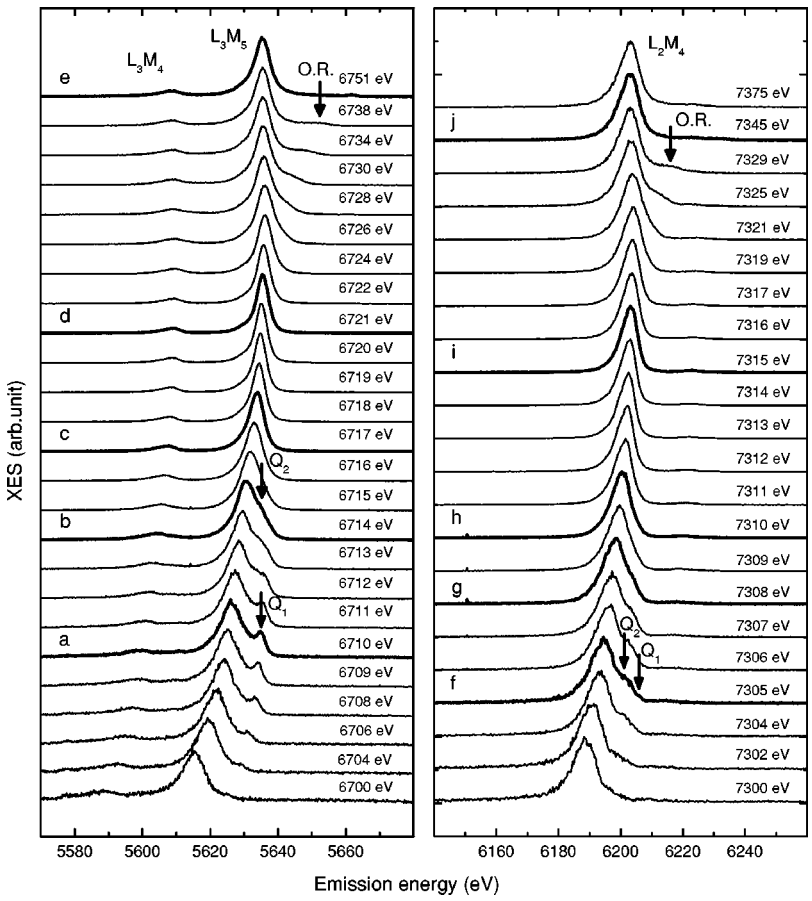

FIG. 2. Incident x-ray energy dependence of RXES spectra for Sm $L_3M_{4,5}$ $(left)$ and Sm $L_3M_{4,5}$ $(right)$. The incident photon energies, at which the spectra were taken, are given in the figure. Labels $a-j$ are consistent with those in Fig. 1. All of the spectra were normalized so that the peak intensity is 1. RXES spectrum peaks labeled Q_1 and Q_2 originate from the $E2$ transitions from $2p$ to $4f$, where Q_1 and Q_2 are attributed to the RXES spectra, which originate from the $E2$ excitation to the majority and minority of the Sm $4f$ spin state, respectively (Ref. 14). The small peak represented as O.R. originates from off-resonant Raman scattering.

$$F(\omega_1,\omega_2)=\sum_f \left|\sum_i \frac{\langle f|T_2|i\rangle\langle i|T_1|g\rangle}{E_i-E_g-\omega_1-i\Gamma_i}\right|^2 \times L(E_f+\omega_2-E_g-\omega_1,\Gamma_f), \quad (3)$$

where $|g\rangle$, $|i\rangle$, $|f\rangle$ are the ground, intermediate, and final states with energies E_g, E_i, and E_f, respectively, ω_1 and ω_2 are the energies of the incoming and outgoing x rays, T_1 and T_2 correspond to the transition operators in the excitation and the radiative decay processes. We take T_1 as the electric dipole transition operator $(\mathbf{e}\cdot\mathbf{r})$ and the electric quadrupole one $(\mathbf{k}\cdot\mathbf{r})(\mathbf{e}\cdot\mathbf{r})$, and T_2 as the electric dipole one $(\mathbf{e}^*\cdot\mathbf{r})$. $L(x,\Gamma)$ is a Lorentzian defined by $L(x,\Gamma)=\Gamma/\pi(x^2+\Gamma^2)$, $\Gamma_i(\Gamma_f)$ is the $2p$ $(3d)$ core hole lifetime broadening of the $L(M)$ shell, which is set to be 2.0 eV (0.5 eV), and all calculated spectra are convoluted by the Gaussian function with the half width at the half maximum, 0.5 eV, as the instrumental resolution.

In a calculation of the electric dipole transition matrix element in the excitation process, we took into account an enhancement effect using a model proposed by Matsuyama *et al.* in the MCD of x-ray-absorption spectroscopy.[11] We took the directions of the incoming and outgoing x rays and the magnetic field in a way consistent with the experimental condition. The electronic configuration, apart from the conduction electrons, of the final state is $3d^94f^5$ for the electric dipole excitation and $3d^94f^6$ for the electric quadrupole one in Sm^{3+}. We took into account the atomic multiplet effect due to the $3d$ spin-orbit coupling and the Coulomb and ex-

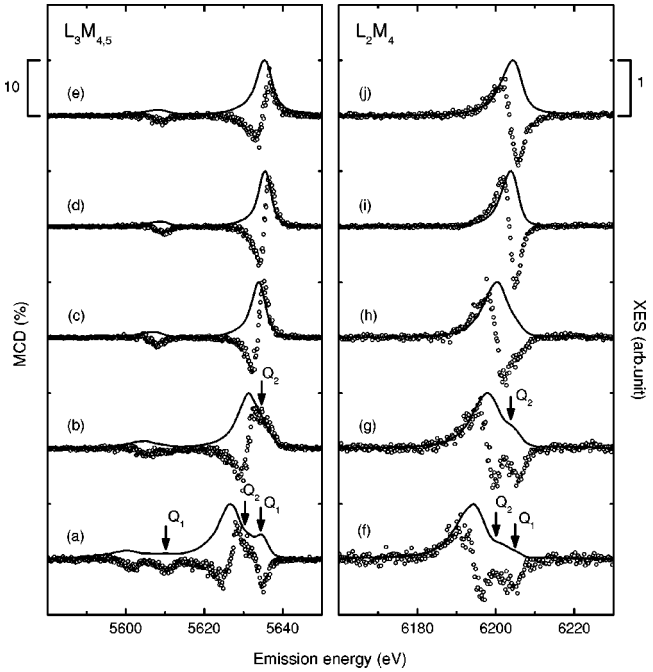

FIG. 3. Measured RXES (solid lines) and MCD spectra (open circles) for Sm $L_3M_{4,5}$ $(left)$ and Sm L_2M_4 $(right)$. Labels $a-j$ are consistent with those in Fig. 1. MCDRXES spectra were normalized by $P_c\cos\theta$.

change interactions among the $3d$ core hole and the $4f$ electrons represented by the Slater integrals.[35] The values of the spin-orbit coupling constants and the Slater integrals are given in Table I. The $4f$ state in the ground state is in the Hund's rule lowest state of the f^5 system ($M_L=5$, $M_s=-5/2$). We assume that the $5d$ state has a density of states given by a semi-elliptical shape with a half width of $W=3.5$ eV for each orbital and spin state (see Ref. 13), further, one electron is occupied in the $5d$ bands. We also assumed a continuum d band with a constant rectangular density of states to reproduce the fluorescencelike component in the calculated spectra.

Figure 4 represents the calculated spectra of RXES and MCDRXES for Sm $L_3M_{4,5}$ and L_2M_4. The intensity of the calculated spectra was divided by the normalization factor used in Fig. 2, then, was renormalized so as to coincide with the experimental spectrum at the center of the white-line resonance, which is $\omega_1=6721$ eV and $\omega_1=7315$ eV for $L_3M_{4,5}$ and the L_2M_4, respectively. The intensities of the calculated spectra except for *d* and *i*, which are used for the normalization, are smaller than the experimental ones. However, the overall agreement of the spectral shapes between the calculated and experimental values is satisfactory for all of the calculated spectra. Thus, the calculated spectra have well explained the detailed $E2$ features for spectra *a* and *b* for $L_3M_{4,5}$ and *f* and *g* for L_2M_4.

The calculated MCDRXES spectra are shown below those of RXES in Fig. 4. The normalization of the calculated MCDRXES spectra is consistent with that of the series of RXES in Fig. 3. The features of all the measured MCDRXES in Fig. 3 are well reproduced by the calculated ones in Fig. 4. Especially, the existence of the $E2$ parts of the MCD, which can be observed for the MCDRXES spectra labeled *a*, *b*, *f*, and *g* in Fig. 3, could be confirmed by the present calculation.

IV. DISCUSSION AND SUMMARY

The present study for Sm $L_3M_{4,5}$ and L_2M_4 was the first one reported in which the $E2$ contribution of MCDRXES was studied for light RE elements. After the previous RXES study by Bartolomé *et al.*[14], Q_1 and Q_2 were characterized as $E1$ radiative decay following $E2$ excitation to the majority and minority levels of the $4f$ state, respectively. It has also been confirmed that the Q_1 peak is observed only in light RE elements because the whole majority level is occupied in heavy RE elements, according to Hund's rule. Since the majority spin corresponds to spin down when we take the quantum axis along the external magnetic field, we observed a single MCDRXES peak with a negative sign for Q_1. Then, the sign of Q_2 MCDRXES is opposite to that for Q_1. These features for Q_1 and Q_2 are completely different from the dispersive spectral shape for $E1$ MCDRXES. On the other hand, comparing MCDRXES and MCDXAS, the signs of the preedge peaks *a* and *b* in Fig. 1 are consistent with those of Q_1 and Q_2 in Fig. 3, respectively. As in the L_3 edge, the preedge structure of MCDXAS has the same sign as that of Q_1 at the L_2 edge in Fig. 3. Judging from Fig. 3(g), the positive $E1$ MCD and the negative $E2$ MCD cancel each other at *g* in Fig. 1. Thus, it has also been confirmed that the result for MCDRXES is favorably consistent with that for MCDXAS.

TABLE I. Spin-orbit coupling constants ξ (eV) of the core nl ($=2p,3d$) and $4f$ orbitals and Slater integrals $F^k=F^k(nl,4f)$, $G^k=G^k(nl,4f)$ (eV) of the nl-$4f$ and $4f$-$4f$ interactions using a Hartree-Fock based program (Ref. 35) for the configurations in the intermediate ($nl=2p$) and final ($nl=3d$) states. The calculations have been carried out using an 80% reduction of all Slater integrals.

	$2p^54f^5$	$3d^94f^5$	$2p^54f^6$	$3d^94f^6$
ξ_{nl}	413.482	10.506	413.529	10.510
ξ_{4f}	0.195	0.195	0.180	0.180
F^2	15.193	15.317	14.251	14.393
F^4	9.590	9.678	8.950	9.049
F^6	6.916	6.982	6.441	6.515
F^2	1.925	9.631	1.790	9.014
F^4		4.495		4.171
G^1	0.199	6.878	0.182	6.357
G^3	0.128	4.032	0.117	3.724
G^5		2.785		2.572

We would like to emphasize the importance of experimental observations of MCDXAS, RXES, and especially MCDRXES in order to detect a weak signal of the $2p$-to-$4f$ $E2$ excitation. As can be seen at the L_3 edge in Fig. 1, the $E2$ signal is invisible in conventional XAS, but in MCDXAS the contribution of the $E2$ excitation can be observed, as the structures *a* and *b*, although feature *b* is a weak shoulder superposed on the $E1$ contribution. In the RXES spectrum of Fig. 3(a), the $E2$ contributions from Q_1 and Q_2 are also detected, but the signal Q_2 is too weak (and superposed on

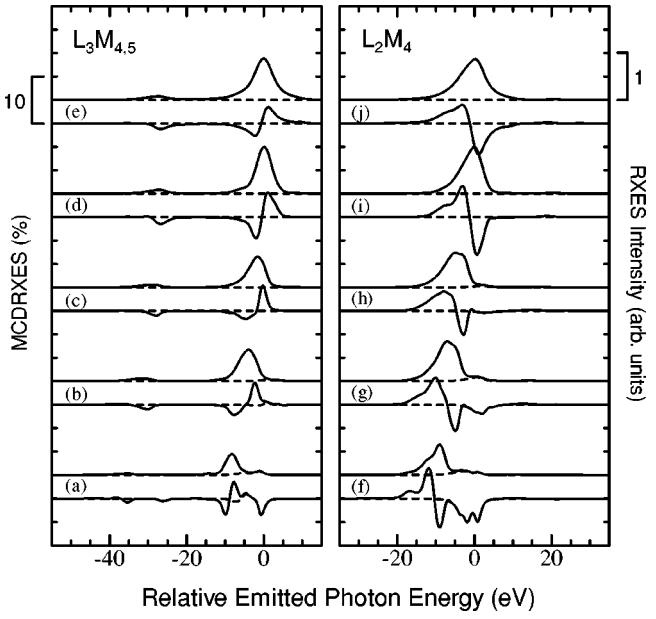

FIG. 4. The calculated RXES (upper) and MCDRXES (downer) for Sm $L_3M_{4,5}$ (*left*) and Sm L_2M_4 (*right*). The dashed lines correspond to the $E2$ part of the spectra. (a)–(j) are consistent with labels *a*–*j* in Fig. 1, respectively.

the $E1$ contribution) to be clearly seen. In order to separate the Q_2 signal from the $E1$ contribution, MCDRXES measurements play an important role. We find in Fig. 3(a) that the Q_2 signal can be clearly seen as a shoulder structure of the MCDRXES spectrum. It might not be evident which of the peak and shoulder in MCDRXES should be assigned as the Q_2 signal, but it is clear from the theoretical calculation shown in Fig. 4(a) that the Q_2 contribution gives rise to the shoulder, while the $E1$ contribution results in the dispersive spectral shape. The remarkable point of our result is that the observation of the negative peak and the positive shoulder of MCDRXES for the Q_1 and Q_2 signals is the direct identification of the $E2$ MCD at the preedge region, and is exactly what we expected to obtain in the present experiment.

It is to be mentioned that the energy separation between Q_1 and Q_2 obtained here (about 4 eV) is smaller than the corresponding value (about 5 eV) obtained by F. Bartolomé *et al.*[14]. Furthermore, Nakazawa *et al.*[36] recently pointed out, with an Nd^{3+} system as an example, that the energy separation between two features by the $E2$ excitation can be somewhat different in XAS, MCDXAS and RXES. For instance, the energy separation between *a* and *b* (MCDXAS) is determined mainly by the $4f-4f$ interaction, while that between Q_1 and Q_2 (RXES) is determined not only by the $4f-4f$ interaction, but also by the $3d$-$4f$ interaction because of the creation of a $3d$ core hole in the final state. A more detailed discussion on these energy separations in the present system will be a problem left for future investigations.

Next, we briefly mention on inconsistency in the RXES intensity between the experimental and theoretical results in Figs. 3 and 4. As a consequence of the present normalization for the calculated RXES intensities, the calculated intensities seemed to be underestimated compared to the experimental values. This may have come from a self-absorption effect, which is strong on the resonant condition and suppresses the RXES intensity. This explanation is supported by the fact that the underestimation can be well compensated using the intensity ratio between absorption and emission, where emission intensity corresponds to the normalization factor used in Fig. 2. Therefore, it is hoped that the coincidence becomes better if the XES intensity without self-absorption effect could be used to normalize the calculated XES. It should be noticed that the magnitude of the magnetic field applied to the sample was different between the MCDXAS and MCDRXES experiments. Applying a magnetic field of 0.6 T to the sample, the magnetization reached more than 96% of that by 1.1 T, at which point the magnetization almost saturated. Thus, the difference in the field seems not to generate any significant problem for a comparison between them. On the other hand, one should pay attention to the difference of θ between the two experiments. The angles of $\theta=45°$ and $\theta=36.9°$ were used for the MCDXAS and MCDXES experiments, respectively. In MCDXAS, θ is associated with the intensity ratio between the $E2$ and the $E1$ contributions. Judging from previous reports on MCDXAS, however, no one could observe the obvious difference in the intensity of MCDXAS depending on θ at room temperature. Although we have not examined the θ dependence of the spectral features of MCDXAS, it is natural to think that we will also not observe it. Therefore, it seems to be possible that we replace the MCDXAS for $\theta=45°$ to that for $\theta=36.9°$ approximately in order to compare the MCDXAS with the MCDRXES measured at $\theta=36.9°$.

In summary, we have studied MCDRXES for the $L_3M_{4,5}$ and the L_2M_4 optical processes in a $Sm_{21}Co_{79}$ amorphous alloy. We succeeded in observing isolated negative and positive peaks of MCDRXES for Q_1 and Q_2, which originate from $E2$ excitation to the majority and minority of the Sm $4f$ spin state, respectively. This result has become a direct identification of $E2$ MCD at the preedge region. Their feature has also explained the spectral shapes of the $E2$ part of MCDXAS very well. We performed a theoretical calculation based on a formula of the coherent second-order optical process, and obtained good agreements with all of the measured MCDRXES spectra.

ACKNOWLEDGMENTS

The authors would like to thank H. Kobayashi of Shin-Etsu Chemical Co. Ltd. for designing the Nd-Fe-B magnetic circuit used in the present experiment. They are grateful to Y. Watanabe, H. Ohsawa, and Dr. M. Mizumaki for their experimental help. This work was performed with the approval of the Photon Factory Program Advisory Committee (Proposal No. 2000G008), and was supported by Grant-in-Aid for Scientific Research from the Japanese Ministry of Education, Science, Sports and Culture.

*Present address: Japan Synchrotron Radiation Research Institute, 1-1-1 Kouto, Mikazuki-cho, Sayo-gun, Hyogo 679-5198, Japan. Electronic address: naka@spring8.or.jp

†Present address: RIKEN Harima Institute, 1-1-1 Kouto, Mikazuki-cho, Sayo-gun, Hyogo 679-5148, Japan.

[1] For example, J.J.M. Franse and R.J. Radwa̧oski, in *Handbook of Magnetic Materials*, edited by K.H.J. Buschow (Elsevier, New York, 1993), Vol. 7.

[2] P. Carra and M. Altarelli, Phys. Rev. Lett. **64**, 1286 (1990).

[3] P. Fischer, G. Schütz, S. Stähler, and G. Wiesinger, J. Appl. Phys. **69**, 6144 (1991).

[4] J.C. Lang, S.W. Kycia, X.D. Wang, B.N. Harmon, A.I. Goldman, D.J. Branagan, R.W. McCallum, and K.D. Finkelstein, Phys. Rev. B **46**, 5298 (1992).

[5] K. Shimomi, H. Maruyama, K. Kobayashi, A. Koizumi, H. Yamazaki, and T. Iwazumi, Jpn. J. Appl. Phys., Suppl. **32**, 314 (1993).

[6] P. Fischer, G. Schütz, S. Scherle, M. Knülle, S. Stähler, and G. Wiesinger, Solid State Commun. **82**, 857 (1992).

[7] J.C. Lang, X. Wang, B.N. Harmon, A.I. Goldman, K.W. Dennis, R.W. McCallum, and K.D. Finkelstein, Phys. Rev. B **50**, 13 805 (1994).

[8] J.C. Lang, G. Srajer, C. Detlefs, A.I. Goldman, H. König, X. Wang, B.N. Harmon and R.W. McCallum, Phys. Rev. Lett. **74**, 4935 (1995).

[9] C. Giorgetti, E. Dartyge, C. Brouder, F. Baudelet, C. Meyer, S. Pizzini, A. Fontaine, and R.M. Galéra, Phys. Rev. Lett. **75**, 3186 (1995).

[10] J. Chaboy, F. Bartolomé, L.M. García, and G. Cibin, Phys. Rev. B **57**, R5598 (1998).
[11] H. Matsuyama, I. Harada, and A. Kotani, J. Phys. Soc. Jpn. **66**, 337 (1997).
[12] M. van Veenendaal, J.B. Goedkoop, and B.T. Thole, Phys. Rev. Lett. **78**, 1162 (1997).
[13] K. Fukui, H. Ogasawara, A. Kotani, I. Harada, H. Maruyama, N. Kawamura, K. Kobayashi, J. Chaboy, and A. Marcelli, Phys. Rev. B **64**, 104405 (2001).
[14] F. Bartolomé, M.H. Krisch, D. Raoux, and J-M. Tonnerre, Phys. Rev. B **60**, 13 497 (1999).
[15] K. Hämäläinen, C.C. Kao, J.B. Hastings, D.P. Siddons, L.E. Berman, V. Stojanoff, and S.P. Cramer, Phys. Rev. B **46**, 14 274 (1992).
[16] S. Tanaka, K. Okada, and A. Kotani, J. Phys. Soc. Jpn. **63**, 2780 (1994).
[17] M.H. Krisch, C.C. Kao, F. Sette, W.A. Caliebe, K. Hämäläinen, and J.B. Hastings, Phys. Rev. Lett. **74**, 4931 (1995).
[18] M. van Veenendaal, P. Carra, and B.T. Thole, Phys. Rev. B **54**, 16 010 (1996).
[19] P.W. Loeffen, R.F. Pettifer, S. Müllender, M.A. van Veenendaal, J. Röhler, and D.S. Silvia, Phys. Rev. B **54**, 14 877 (1996).
[20] J.J. Gallet, J.M. Mariot, L. Journel, C.F. Hague, A. Rogalev, H. Ogasawara, A. Kotani, and M. Sacchi, Phys. Rev. B **60**, 14 128 (1999).
[21] M.H. Krisch, F. Sette, U. Bergmann, C. Masciovecchio, R. Verbeni, J. Goulon, W. Caliebe, and C.C. Kao, Phys. Rev. B **54**, R12 673 (1996).
[22] T. Iwazumi, K. Kobayashi, S. Kishimoto, T. Nakamura, S. Nanao, D. Ohsawa, R. Katano, and Y. Isozumi, Phys. Rev. B **56**, R14 267 (1997).
[23] T. Nakamura, S. Nanao, T. Iwazumi, K. Kobayashi, S. Kishimoto, D. Ohsawa, R. Katano, and Y. Isozumi, J. Electron Spectrosc. Relat. Phenom. **92**, 261 (1998).
[24] T. Iwazumi, T. Nakamura, H. Shoji, K. Kobayashi, S. Kishimoto, R. Katano, Y. Isozumi, and S. Nanao, J. Phys. Chem. Solids **61**, 453 (2000).
[25] T. Iwazumi, K. Kobayashi, T. Tominaga, T. Nakamura, S. Nanao, S. Kishimoto, D. Ohsawa, R. Katano, and Y. Isozumi, J. Synchrotron Radiat. **6**, 685 (1999).
[26] K. Fukui, H. Ogasawara, A. Kotani, T. Iwazumi, H. Shoji, and T. Nakamura, J. Phys. Soc. Jpn. **70**, 1230 (2001).
[27] K. Fukui, H. Ogasawara, A. Kotani, T. Iwazumi, H. Shoji, and T. Nakamura, J. Phys. Soc. Jpn. **70**, 3457 (2001).
[28] T. Nakamura, N. Kawamura, T. Iwazumi, H. Maruyama, A. Urata, H. Shoji, S. Nanao, S. Kishimoto, R. Katano, and U. Isozumi, J. Synchrotron Radiat. **8**, 428 (2001).
[29] T. Iwazumi, K. Kobayashi, S. Kishimoto, T. Nakamura, S. Nanao, D. Ohsawa, R. Katano, Y. Isozumi, and H. Maruyama, J. Electron Spectrosc. Relat. Phenom. **92**, 257 (1998).
[30] T. Nakamura, H. Shoji, S. Nanao, T. Iwazumi, S. Kishimoto, R. Katano, and Y. Isozumi, Phys. Rev. B **62**, 5301 (2000).
[31] F.M.F. de Groot, M. Nakazawa, A. Kotani, M.H. Krisch, and F. Sette, Phys. Rev. B **56**, 7285 (1997).
[32] T. Jo and A. Tanaka, J. Phys. Soc. Jpn. **67**, 1457 (1998).
[33] K. Fukui, H. Ogasawara, I. Harada, and A. Kotani, J. Synchrotron Radiat. **8**, 407 (2001).
[34] T. Iwazumi, A. Koyama, and Y. Sakurai, Rev. Sci. Instrum. **66**, 1691 (1995).
[35] R.D. Cowan, *The Theory of Atomic Structure and Spectra* (University of California Press, Berkeley, 1981).
[36] M. Nakazawa, K. Fukui, H. Ogasawara, A. Kotani, and C.F. Hague, Phys. Rev. B **66**, 113104 (2002).